ACS APPLIED POLYMER MATERIALS

pubs.acs.org/acsapm Article

Current Response Enhancement According to the Doping Anion's Nature in Redox Polyelectrolyte—Enzyme Assemblies

Lucy L. Coria-Oriundo, Santiago E. Herrera, Lucila P. Méndez De Leo, and Fernando Battaglini*

Cite This: https://doi.org/10.1021/acsapm.2c01300 Read Online

ACCESS | Metrics & More | Article Recommendations | Supporting Information

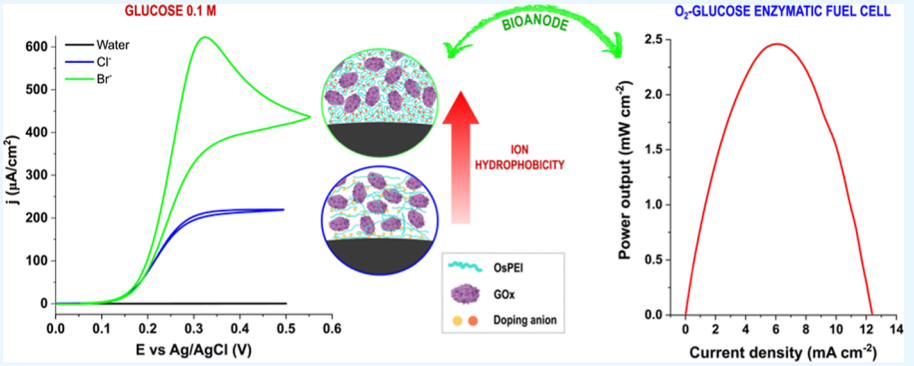

ABSTRACT: High-power density output in enzymatic fuel cells is a key feature to reduce the size of self-powered implantable medical devices. Electron transfer mediated through redox polyelectrolytes allows the transport of electrons from enzymes away from the electrode, improving the current output. It is known that doping ions in polyelectrolytes introduce relevant characteristics in the generation of assemblies regarding mass adsorption and stiffness. In this work, binary 1:1 sodium salts (NaX; X = F^-, Cl^-, Br^-, NO_3^-, ClO_4^-) were studied as doping ions of two redox polyelectrolytes (osmium-based branched polyethyleneimine and osmium-based linear polyallylamine) to enhance the adsorption and electron transfer process in glucose oxidase/redox polyelectrolyte assemblies. Cyclic voltammetry, polarization modulation infrared reflection absorption spectroscopy, quartz crystal microbalance with dissipation, and atomic force microscopy were used to understand the growth mechanism of these films and their performance. Ion hydrophobicity plays a key role, bromide being the one that generates the greater absorption and the best electron transfer efficiency for both redox polyelectrolytes. Branched polyethyleneimine doped with bromide was the best combination for the construction of bioanodes. Its application on an O_2−glucose enzymatic fuel cell yields a power density output of 2.5 mW cm^{-2}, achieving state-of-the-art performance.

KEYWORDS: *doped polyelectrolyte, hydrophobic ion, redox hydrogel, mediated electron transfer, bioanode*

INTRODUCTION

Oxidoreductases are a kind of enzyme able to catalyze reduction and oxidation reactions in nature. The comprehension of the mechanisms involved in these reactions allows for their use in different applications, such as biosensors and biofuel cells.[1,2] A key point in these applications is a rapid electron transfer process from a soluble substrate to an electrode surface, which is sometimes overshadowed by the size of the enzyme, restricting its direct reaction with the electrode. To overcome this impediment, redox mediators which are small molecules stable in both oxidation states and able to undergo a rapid electron transfer process with the redox enzyme and the electrode are used. This process is called mediated electron transfer (MET).[3]

A convenient way to generate a stable immobilized system involving the enzyme, the mediator, and the electrode, and which in turn guarantees an efficient electron transfer process, is the use of mediators bound to polyelectrolytes, which behave as a redox hydrogel. Due to the progress made in the knowledge of the properties and reactions involving polyelectrolytes,[4−6] new strategies regarding the casting to obtain stable and efficient hydrogels continue to emerge.[7]

Protein−polyelectrolyte assemblies in multilayers have shown to be a relevant issue in areas such as biosensing, biocatalysis, and drug delivery.[8,9] In their buildup process, the growth and stability of these systems are highly affected by the ionic strength of the used solutions. Most works have paid attention to the concentration, mainly involving chloride ions,

Received: July 27, 2022
Accepted: September 13, 2022

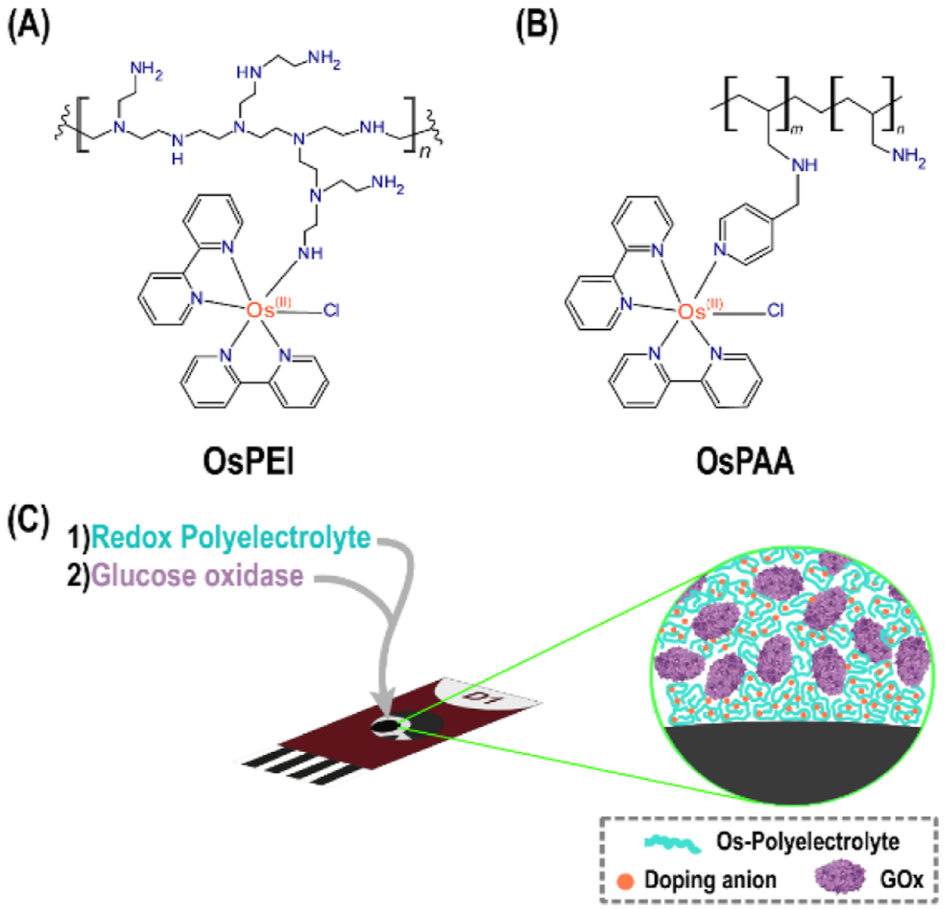

Figure 1. Chemical structures of osmium-modified polyelectrolytes: (A) OsPEI and (B) OsPAA. (C) Scheme of the osmium-modified polyelectrolyte@NaX/GOx@H_2O LbL assembly system with X = F^-, Cl^-, Br^-, NO_3^-, or ClO_4^- over an in-house screen-printed graphite electrode.

analyzing the results in terms of the charges surrounding the protein and the polyelectrolyte.[10−13] However, the nature of the ion also plays a role as it is already known through the Hofmeister series, where ions are ordered based on their capability to alter the solubility of the proteins and polyelectrolytes.[14−16] In this regard, the ability of a given salt to enhance a property in a hydrogel has been proven. For example, the generation of ductile and strong hydrogels in the presence of ammonium sulfate,[17] the use of weakly hydrated anions to solubilize hydrophobic macromolecules,[18] sodium citrate to produce multilength-scale hierarchical hydrogel architectures,[19] and the effect of different ions on the properties of polyelectrolyte complexes[6] are just a few of the recent works using the nature of small ions to shape the properties of a hydrogel. However, little is known about their impact on the electron transport process in redox hydrogels.

Here, we explore the effect of different anions (F^-, Cl^-, Br^-, NO_3^-, and ClO_4^-) on the buildup and electron transfer process of a layer by layer (LbL) redox-enzyme/redox-polyelectrolyte system [a glucose oxidase−osmium complex bound to polyethyleneimine (PEI) or polyallylamine (PAA)]. Our data show that the nature of the anion present in the process has an important impact on the amount of the loaded material after each deposition. The system containing bromide exhibits the best electrocatalytic response, and it was used in the construction of an enzymatic fuel cell displaying competitive results compared to those presented in the literature.

MATERIALS AND METHODS

Reagents and Materials. $OsCl_6(NH_4)_2$, pyridine aldehyde (pyCHO), sodium cyanoborohydride (cat #156159), branched PEI (cat #408727), and PAA (cat #479136) were procured from Sigma-Aldrich; 2,2′-bipyridine (bpy) was provided by Fluka. Glucose oxidase (GOx) was procured from Aspergillus Niger, Calzyme Laboratories, Inc. All other reagents were of analytical grade. Ultrapure water (18 MOhm) was used to prepare the solutions.

Redox Polyelectrolyte Synthesis. The complex [$Os(bpy)_2Cl$-(PyCHO)]Cl was synthesized as previously reported by Kober et al.[20] The osmium-modified branched PEI (OsPEI) was synthesized as previously reported.[21] The osmium-modified PAA (OsPAA) was synthesized by adapting the procedure reported by Hermanson.[22] 1 mg/mL PAA and 4.6 mM osmium complex in 0.2 M carbonate/bicarbonate buffer solutions at pH 9.6 were prepared. These solutions were mixed to obtain a complex/amine molar ratio of 1:3.7 and left for 2 h at room temperature. Then, a 5 M sodium cyanoborohydride solution was added to a 1:10 complex/cyanoborohydride molar ratio and left for 1 h at room temperature. The unreacted osmium complex was removed by dialysis using a 3 kDa cutoff membrane against water acidified at pH 3.0 with HCl. The osmium complex content was determined by measuring its absorbance at 490 nm.

Graphite Electrode Modification. A screen-printed three-electrode system with graphite working electrodes was used.[23] The electrodes were modified by alternating exposure to solutions of redox polyelectrolytes (0.48 mM in osmium, OsPEI, or OsPAA, dissolved in water or sodium salts at pH 7.0) and GOx (1 mg mL^{-1}, water, pH 7.0). Electrodes were modified following the procedure previously described by Coria-Oriundo et al.[21]

Electrochemical Experiments. Cyclic voltammetry measurements were carried out in solution containing a 50 mM 4-(2-

https://doi.org/10.1021/acsapm.2c01300
ACS Appl. Polym. Mater. XXXX, XXX, XXX−XXX

hydroxyethyl)-1-piperazineethanesulfonic acid (HEPES) + 100 mM NaCl buffer solution at pH 7.0 or in 100 mM glucose in 50 mM HEPES + 100 mM NaCl using a purpose-built potentiostat (TEQ-04, NanoTeq, Buenos Aires, Argentina). Carbon cloth (Morgan Specialty Graphite, National Electric Carbon Products, Greenville, South Carolina, USA) electrodes were activated with a 1:1 isopropanol/water solution and washed with Milli-Q water. Two-compartment biofuel cells were constructed using the carbon cloth electrode modified following the same procedure for graphite electrodes and a high-platinum-loading gas diffusion electrode (HLDGE, 4 mg cm^{-2} Platinum Black-Cloth, FuelCellsEtc, College Station, Tx, USA). The modified carbon cloth electrode was immersed in 100 mM glucose in a 50 mM HEPES + 100 mM NaCl solution. The HLDGE was immersed in 0.1 M $HClO_4$, and oxygen was bubbled through the solution until saturation. The electrode−electrolyte systems were connected through a fritted glass. Scan polarization was carried out as previously reported by Coria-Oriundo et al.[21]

Quartz Crystal Microbalance Measurements. The quartz crystal microbalance with dissipation (QCM-D) experiments were performed, using redox polyelectrolyte and enzyme solutions as described for graphite electrode modification, following a procedure previously reported.[21]

IR Spectroscopy. Polarization modulation infrared reflection absorption spectroscopy (PM-IRRAS) experiments were performed following a procedure previously reported.[24] The gold substrate was modified following the same procedure as that described for graphite electrode modification.

Atomic Force Microscopy. An Agilent 5500 atomic force microscope/scanning probe microscope was used for atomic force microscopy (AFM). Contact mode and tapping mode measurements were carried out using insulating Si PointProbe Plus PPP-CONT tips (<10 nm tip radius, a force constant of 0.2 N/m, a resonance frequency of 13 kHz) and PointProbe Plus PPP-NCL tips (<10 nm tip radius, a force constant of 48 N/m, a resonance frequency of 190 kHz), respectively. While the topography of single polyelectrolyte layers was studied over highly oriented pyrolytic graphite (HOPG) in the tapping mode, the topography of multilayer redox polyelectrolyte/GOx was studied over H_2-flamed annealed Arandee Robax Au surfaces in the contact mode. Mean film thicknesses were calculated by extracting a one-dimensional (1D) distribution of heights of a flattened AFM image exposing equal amounts of the surface and film and calculating the distance between the peak corresponding to the surface and the peak corresponding to the film. The roughness average parameter was calculated along a 1 μm straight line over a surface-representative AFM image. All images were analyzed using Gwyddion V2.49 (http://gwyddion.net/).

RESULTS

We performed the sequential adsorption of an osmium modified-polyamine and glucose oxidase (GOx) enzyme over a graphite electrode using the LbL technique. This methodology allows one to create an enzymatic hydrogel at the interface of the electrode that can be further utilized as a bioanode. Two redox polyelectrolytes were investigated, one branched (OsPEI, Figure 1A) and the other linear (OsPAA, Figure 1B).

OsPEI-GOx Assemblies. The LbL surface modification was performed by controlling the ionic strength conditions in each of the steps of the process. Different anion types and concentrations, always as sodium salts, were used in the presence of the redox polyelectrolyte during the adsorption process on the electrode surface. The washing process was performed with ultrapure water. The step corresponding to the enzyme adsorption was carried out in the absence of salts. In this way, different assemblies were built in the presence of 0.2 M sodium salts of the corresponding anions on a three-electrode screen-printed system (Figure 1C).

After electrode modification, the electrochemical performance was evaluated in the absence of glucose. Cyclic voltammetry displayed the typical electrochemical response of a reversible redox process centered at 0.30 V corresponding to the osmium center tethered to the surface. In the presence of glucose, the anodic current density increases, reaching a catalytic plateau corresponding to the osmium-mediated glucose oxidation through GOx.

The effect of the absence and the presence of glucose on the electron transfer process is shown in Figure 2 and compared to

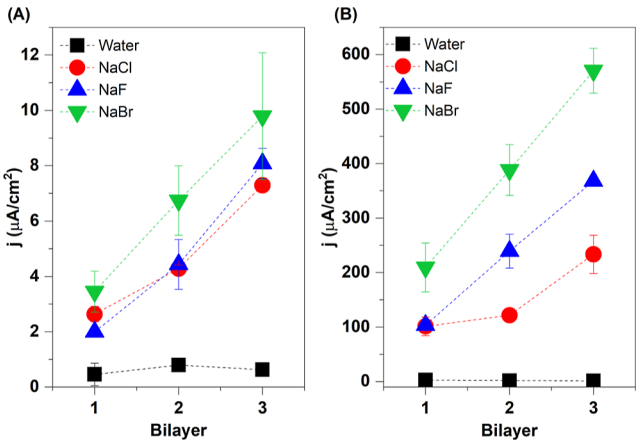

Figure 2. (A) Cyclic voltammograms after deposition of each bilayer (OsPEI@NaX/GOx@H_2O) without glucose. (B) Maximum catalytic current densities in the presence of 100 mM glucose. Scar rate: 10 mV s^{-1}. Buffer: 50 mM HEPES + 0.1 M NaCl, pH 7.0.

an OsPEI/GOx system that was constructed without adding any salt (black squares). In the absence of glucose (Figure 2A), the current response increased as the number of bilayers increased for all anions following a linear behavior. When the polyelectrolyte is adsorbed in the absence of a salt, an almost constant current density lower than 1 μA cm^{-2} is observed. Current densities for systems using Cl^- and F^- in OsPEI solutions were similar for the three bilayers and slightly higher for Br^-. Also, the buildup process was studied in the presence of NO_3^- and ClO_4^-. These results are not presented in this figure since the values obtained for NO_3^- were similar to those for Br^- (see Supporting Information, Figure S1), while the addition of ClO_4^- to OsPEI yielded a precipitate under these conditions.[25]

In the presence of glucose (Figure 2B), the difference in the behavior of the LbL systems built in the presence of different salts is more noticeable and follows the same trend: as the number of bilayers increases, a greater amount of the polyelectrolyte is exposed for GOx adsorption, and higher catalytic current densities are observed. In contrast, the assembly grown without any salt shows low catalytic current densities and decreases with an increasing number of bilayers.

To discern if this tendency was due to a stronger interaction between the enzyme and polyelectrolyte or simply a major amount of GOx adsorbed, the growth of the LBL assemblies was analyzed with a QCM-D to evaluate the adsorbed mass and the changes in the stiffness of the films. The results are shown in Figure 3. For the first bilayer, the adsorbed mass increased; however, exposure to the OsPEI solution resulted in a slight decrease in the mass, followed by an important increase when the film was then exposed to GOx again. The same

https://doi.org/10.1021/acsapm.2c01300
ACS Appl. Polym. Mater. XXXX, XXX, XXX−XXX

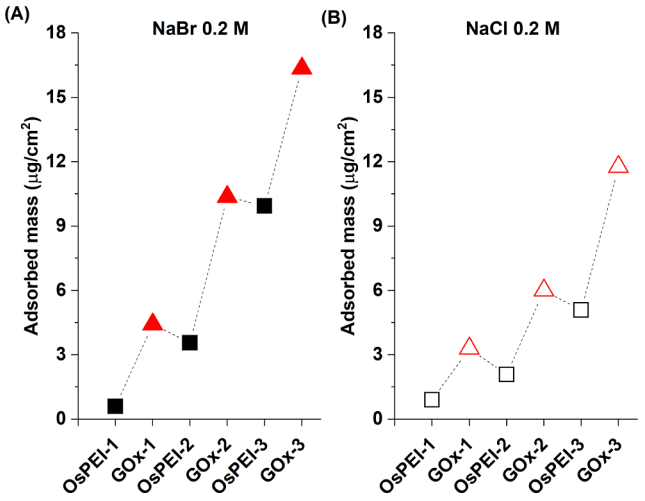

Figure 3. QCM-D experiments: adsorbed mass for OsPEI/GOx using OsPEI solutions with (A) 0.2 M NaBr or (B) 0.2 M NaCl.

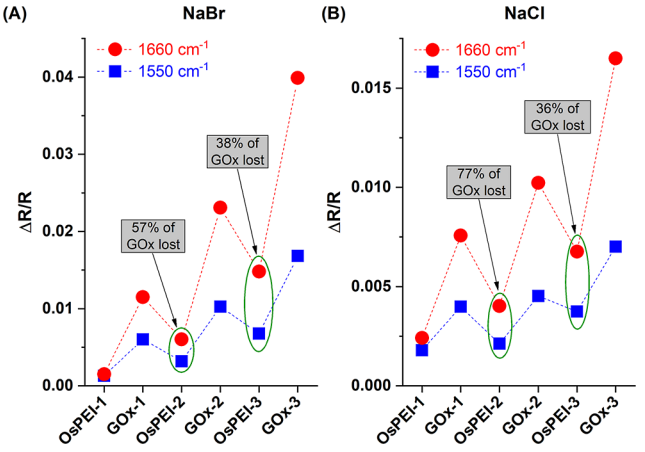

Figure 4. PM-IRRA spectra: variation in the intensities of the main signals as a function of layer increment. OsPEI solutions with (A) 0.2 M NaBr or (B) 0.2 M NaCl.

pattern was observed for the third bilayer. This behavior could suggest that OsPEI was not adsorbed, and a part of GOx was desorbed from the film. Nevertheless, as seen in Figure 2A, the peak current density for these assemblies increased with each OsPEI layer, verifying that more OsPEI was adsorbed in the following layers, indicating that the presence of salt in the polyelectrolyte-adsorption step partially removed the enzyme.

To follow the adsorption/desorption of GOx from the film, its growth was also studied using PM-IRRAS. In PM-IRRAS experiments, the adsorbed matter and thin layers on metal surfaces are analyzed in the reflection geometry mode under grazing incidence. In this way, the buildup process was followed through the bands at ∼1660 and ∼1550 cm^{-1} corresponding to vibrations associated with the enzyme[26] (Figure S2A in the Supporting Information shows the spectra obtained through the buildup process). No peaks corresponding to OsPEI were observed, even at high wavenumbers. Hence, these spectra allowed the analysis of the construction of the assemblies exclusively following the enzyme deposition. The PM-IRRA spectra showed a decrease in the peak intensities when the surface was exposed to OsPEI solution in the presence of bromide, for the adsorption of the second and third OsPEI layers, and an increase in the peak intensities when it was exposed to GOx solution. Similar behavior was observed when chloride ions were used as doping ions in OsPEI solutions (Figure S2B). These results follow the trend observed in QCM-D experiments.

Since the spectra signals are dependent on the amount of adsorbed GOx and considering the difference between the intensities of peaks before and after OsPEI deposition, it is possible to estimate the fraction of GOx retained in the film after each OsPEI adsorption. For assemblies using OsPEI solutions with bromide (Figure 4A), when the system was exposed to OsPEI solution to assemble the second OsPEI layer, almost 57% of GOx was desorbed from the surface, while after the third OsPEI layer, about 38% of GOx was lost. The effect of the chloride ion is similar: 77 and 36% of GOx are lost after the second and third OsPEI layers are assembled, respectively (Figure 4B).

If GOx desorbs with its respective hydration water molecules and the difference between peak intensities of the spectra of OsPEI-1/GOx-1 and OsPEI-2/GOx-1 is directly related to the amount of GOx lost from the film, the same mass percentage lost can be considered in QCM-D experiments. Taking this information into account, the QCM-D experiments can be analyzed as follows: for the assembly in the presence of bromide, 0.60 μg of OsPEI and 3.82 μg of GOx are adsorbed at the first bilayer (details are given in Table S1, Supporting Information, page S8). When the surface is exposed to the OsPEI solution for the second OsPEI layer, a fraction of GOx is desorbed. Considering the PM-IRRAS result (57% lost), the amount of GOx lost should have been 2.20 μg. However, the change in mass obtained using QCM-D indicated that only 0.86 μg is lost (Table S1). As this process occurred in the presence of OsPEI, the decrease in the amount of the mass loss can be attributed to a net exchange process: part of the GOx is lost, and some OsPEI is adsorbed. The difference between these values represents the mass of OsPEI adsorbed (1.34 μg). The same analysis was carried out for the following layers, and their results are shown in Table 1. A similar procedure was carried out for the assembly with chloride using the data from QCM-D and PM-IRRAS measurements. In this way, we can estimate the amount of the enzyme and redox polyelectrolyte for each system at any layer (GOx or OsPEI) and the total up to each bilayer (Table 1).

After the three bilayers are assembled, the masses adsorbed of both species, OsPEI and GOx, are found to be almost 6 times higher in the presence of bromide than in the presence of chloride. Additionally, the ratio between GOx/OsPEI is practically the same for both cases (2.4 for Br^- and 2.3 for Cl^-), and the ratios between current densities in the presence and the absence of glucose are 59 and 32 for bromide and chloride, respectively, indicating that the presence of the bromide anion not only promotes a higher adsorption but also promotes a better interaction between the redox mediator and enzyme molecules. This fact can be understood considering that a more flexible film is formed. In the case of the bromide ion, with each OsPEI layer added, the dissipation increases (data shown in Table S1), independent of the sign of the mass change, suggesting a more flexible film.

The results from QCM-D measurements show that a higher mass was adsorbed in the QCM-D sensor when bromide was used, which is in accordance with the higher current density obtained with respect to that of chloride as shown in Figure 2A. These results indicate that the film has a higher content of

https://doi.org/10.1021/acsapm.2c01300
ACS Appl. Polym. Mater. XXXX, XXX, XXX−XXX

Table 1. OsPEI and GOx Adsorbed Masses for Each Deposited Layer and Bilayer of the Assemblies OsPEI/GOx with Bromide and Chloride

		OsPEI@NaBr		OsPEI@NaCl	
bilayer	layer	OsPEI mass (μg cm^{-2})	GOx mass (μg cm^{-2})	OsPEI mass (μg cm^{-2})	GOx mass (μg cm^{-2})
OsPEI-1/GOx-1	OsPEI-1	0.60		0.35	
	GOx-1		3.82		0.94
	total	0.60	3.82	0.35	0.94
OsPEI-2/GOx-2	OsPEI-2	+1.34	−2.20	+0.41	−0.720
	GOx-2		+6.81		+0.977
	total	1.93	8.44	0.76	1.195
OsPEI-3/GOx-3	OsPEI-3	+2.82	−3.25	+0.085	−0.44
	GOx-3		+6.41		+1.20
	total	4.75	11.6	0.85	1.96
	ratio		2.4		2.3

OsPEI due to the presence of a more hydrophobic anion. The same behavior was observed for GOx; a higher mass is adsorbed on the OsPEI film grown in the presence of bromide, which follows the same behavior observed for catalytic current densities (Figure 2B), a trend that continues throughout the assembly.

This effect can be explained considering that a coiled conformation is adopted by the polyelectrolyte due to a higher ion pairing with bromide, a more hydrophobic anion.[27−29] Similar results were reported for polyelectrolyte assemblies involving polystyrenesulfonate (PSS) and PAA.[29,30]

We performed AFM measurements over a single layer of OsPEI (OsPEI-1/GOx-0) adsorbed on HOPG in the presence of Br^- and Cl^- anions to investigate their effect on the structural characteristic of the LbL assembly. Figure 5 shows two main differences: the surface coverage and homogeneity are higher for the OsPEI@NaBr film, and the mean film thickness is almost 2 times higher than that of the OsPEI@NaCl film (2.0 nm for OsPEI@NaCl and 3.7 nm for OsPEI@NaBr). Both results are consistent with the enhanced interaction between the surface and the bromide-doped polymer (note that the incubation time was the same for the two cases). As HOPG is a highly hydrophobic surface,[31] the fact that the bromide-doped polymer interacted more strongly with the surface indicates that the bromide anion increases the hydrophobic character of the polymer. Conversely, when chloride ions are present, only a few isolated polymer chains adsorb over the surface, which is indicative of fewer polymer−surface interactions and a more hydrophilic character.

GOx-containing films were also studied over Au substrates (hydrophilic surface) to match QCM-D experimental conditions. Figure S3A shows AFM images of OsPEI-2/GOx-1 and OsPEI-3/GOx-3 films deposited in the presence of Br^- and Cl^- anions. Although there are no major differences in the surface coverage, as was observed with HOPG, the presence of the bromide ion in the OsPEI film assembly displayed grains of bigger sizes (the polymer−polymer interaction is stronger than the polymer−surface interaction), leaving voids that can be further occupied by GOx, allowing a stronger interaction between the polyelectrolyte and enzyme that in turn improves the electron transport through the film. This feature has a direct correlation with the surface roughness, especially for OsPEI-2/GOx-1 assemblies, as the film exposes both materials, gold and organic matter. The calculated surface roughness was 0.588 and 1.35 nm for OsPEI-2/GOx-1 with chloride and bromide anions, respectively (Figure S3-B). Again, the result is consistent with enhanced hydrophobicity due to the addition of bromide ions.

The effect of the anion concentration on the generated current was evaluated. For chloride, in the absence of glucose (Figure S4A), the current density increases when the salt concentration is varied from 0.2 to 1.0 M and slightly decreases at higher concentrations (2.0 M). The catalytic current response shows a maximum at 0.5 M NaCl and a decrease of ca. 30% at higher concentrations when glucose is present (Figure S4B). On the other hand, with bromide, no significant differences are observed from 0.2 to 0.5 M in any case (Figure S4C,D). However, at a higher concentration (0.8 M), a sharp decrease in current densities is observed.

OsPAA-GOx Assemblies. The presence of chloride, fluoride, and bromide ions at the same concentration was evaluated in OsPAA solutions used for OsPAA/GOx assemblies to compare the effect of these ions on a linear redox polyelectrolyte. OsPAA (Figure 1B) has been widely studied in assemblies with enzymes, incorporating metallic nanoparticles, surfactants, and phosphate ions.[32−34]

In the absence of glucose, the current densities with OsPAA at the first layer were 2 times larger than that with OsPEI (Figure S5A,B), suggesting a greater affinity of this polyelectrolyte to the electrode surface (graphite). Chloride and bromide ions showed similar and higher noncatalytic current densities compared to those of fluoride. Then, the bilayer growth follows a linear trend, with a higher slope compared to that of OsPEI (ca. 3 vs 2 μA cm^{-2} per bilayer). On the other hand, in the presence of glucose, the current response presents the following order: $F^- < Cl^- < Br^-$. Despite OsPAA introducing a greater amount of osmium centers than OsPEI, the catalytic current densities only reach ca. 40% than those obtained with OsPEI even with bromide ions (240 vs 570 μA cm^{-2}).

The OsPAA/GOx assembly in the presence of NaBr was also studied using QCM-D and PM-IRRAS. The adsorbed mass determined by QCM-D experiments (Figure S5C) and the PMIRRAS spectra (Figure S6A) show the same behavior as OsPEI/GOx assemblies, and a decrease was observed in both adsorbed mass and PMIRRAS signals after the second and third OsPAA layers.

Using the variations in PMIRRAS peak intensities (Figure S6B) and the QCM-D data, the GOx and OsPAA adsorbed masses for the second and third bilayers were calculated (Table S2, Supporting Information, Page S9). In the case of OsPAA, the GOx/polyelectrolyte ratio is 14 versus 2.4 for OsPEI. This indicates a greater affinity of OsPAA for GOx, but, at the same

https://doi.org/10.1021/acsapm.2c01300
ACS Appl. Polym. Mater. XXXX, XXX, XXX−XXX

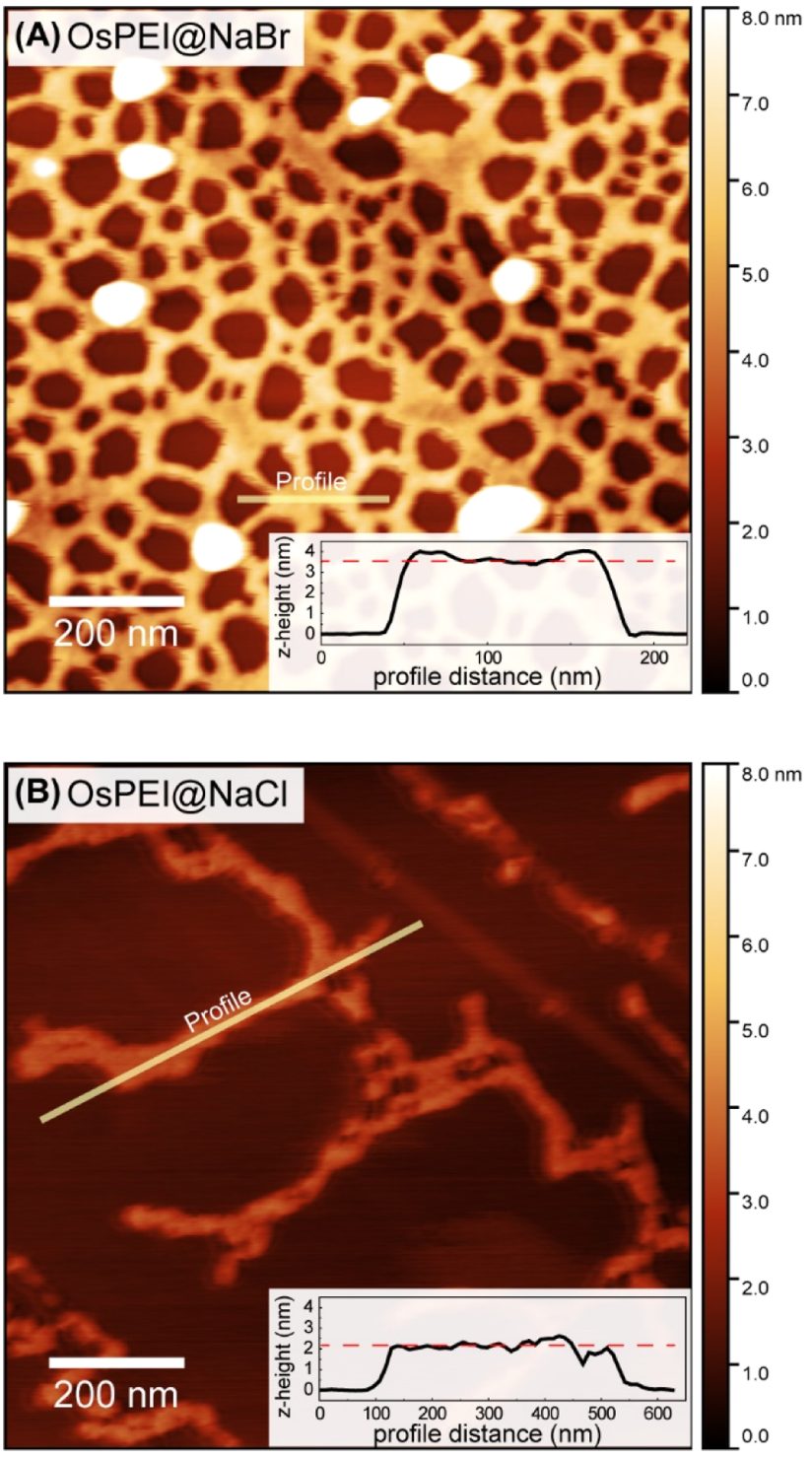

Figure 5. AFM topography images of (A) OsPEI@NaBr and (B) OsPEI@NaCl over HOPG. Insets show height profiles corresponding to selected lines displayed over AFM images.

time, this higher amount of GOx in the system seems to act as an insulator instead of improving the catalytic current (compare Figures 2B and S5-B).

In these experiments, dissipation changes increased with each OsPAA layer, as in the case of OsPEI, but decreased when GOx was adsorbed. These results show that as the LBL system grows, the film becomes more rigid. Therefore, even though the amount of GOx is 14 times the OsPAA mass and the GOx total mass is higher in the presence of OsPAA than OsPEI, the osmium centers and the active sites of the enzyme connect less effectively, generating lower catalytic current densities with OsPAA compared to that with OsPEI. This suggests that the linear backbone of the polyelectrolyte produces a more rigid structure and a thinner film, limiting the interaction between redox moieties in the polyelectrolyte and the enzyme. Therefore, the difference in the electrochemical behavior between OsPAA and OsPEI in the presence of the same hydrophobic anion is due to the higher hydrophobicity of the

https://doi.org/10.1021/acsapm.2c01300
ACS Appl. Polym. Mater. XXXX, XXX, XXX−XXX

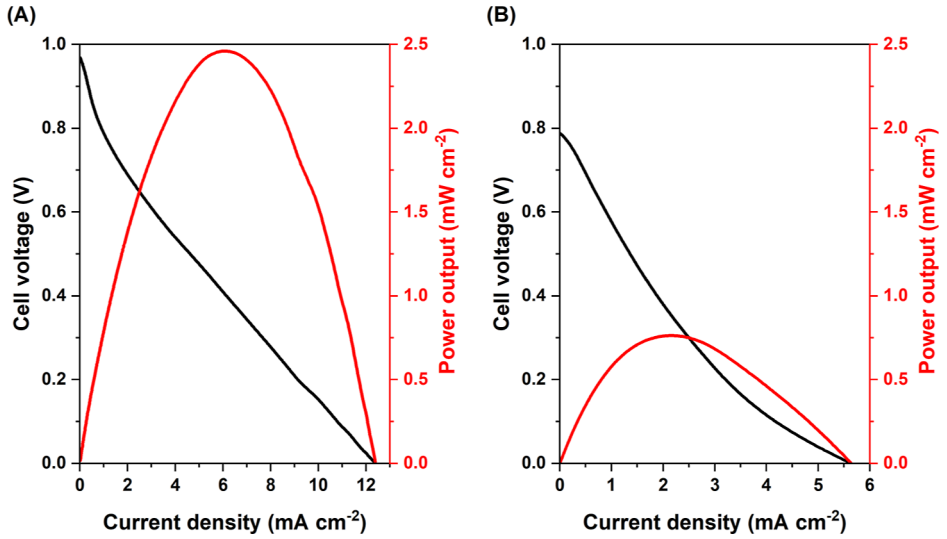

Figure 6. Cell voltage and power output density vs current density for two biofuel cells. Anodes: (A) OsPEI/GOx or (B) OsPAA/GOx assemblies using redox polyelectrolyte solutions in the presence of 0.2 M NaBr. Cathode: a HLDGE.

linear polyelectrolyte and to the difference in the stiffness of the systems that affect the redox interactions.

Enzymatic Fuel Cells. The LbL system built with a branched redox polyelectrolyte in the presence of bromide has shown to be extremely effective since three bilayers can achieve a current density similar to that of systems built with linear polymer containing tethers binding redox centers to linear polymer backbones.[35,36]

Furthermore, the modified electrodes with OsPEI/GOx and OsPAA/GOx assemblies in the presence of NaBr were used as bioanodes in a glucose/oxygen hybrid enzymatic fuel cell. Figure 6 shows the results for the two-compartment biofuel cells. The OsPEI/GOx bioanode shows an open-circuit voltage of 0.97 V, yielding a maximum current density of 12.4 mA cm^{-2} and a power output of 2.5 mW cm^{-2}. Moreover, the OsPAA/GOx bioanode shows an open-circuit voltage of 0.79 V, yielding a maximum current density of 5.6 mA cm^{-2}, and the power output reaches about 0.80 mW cm^{-2}. The higher power output and current density of the OsPEI/GOx bioanode are due to a higher catalytic response of this system in comparison with that of the OsPAA/GOx assembly.

DISCUSSION

The presence of salts in polyelectrolyte solutions has two main effects, the ions can act as counterions of charged units in the polyelectrolyte through ion pairing and as co-ions not forming pairs (Debye screening).[9] The first effect is considered a short-range interaction where the hydrophilic/hydrophobic character of the ion is the main driving force, while the second, considered a long-range interaction, can be modeled by continuum electrostatic. Most of the works related to the effect of ionic strength on the construction of polyelectrolyte−protein multilayers focus on the range of concentrations of a given salt, generally sodium chloride, and the results are explained through an electrostatic model.[9]

In this work, we have used five binary 1:1 sodium salts (NaX; X = F^-, Cl^-, Br^-, NO_3^-, ClO_4^-). A first screening combining OsPEI with 0.2 M NaX shows that the electrochemical response of the films follows a trend $F^- \approx Cl^- < Br^- \approx NO_3^-$, while in the presence of ClO_4^-, the polyelectrolyte precipitates. These similarities and differences among ions have also been observed in the construction of multilayers involving polyelectrolytes of opposite charges.[29,37,38] In particular, El Haitami et al.[29] studied the interaction of different anions with PAA in the buildup of PAA/PSS and its effect on the permeability of electroactive probes. As in our case, they found greater adsorption in the presence of chaotropic anions (NO_3^-, ClO_4^-) related to a loopier conformation.

On the other hand, although F^- and Cl^- have similar hydrophobicity, in our case, the assembly with F^- shows higher currents due to a higher redox polyelectrolyte mass adsorbed. Note that F^- is a highly hydrated ion able to form hydrogen bonds with the polyelectrolyte and water molecules;[5] therefore, different interaction forces should be considered. Considering these results, we decided to focus on chloride and bromide ions to establish the differences that these doping ions can produce in the catalytic current response observed in the presence of glucose.

Both anions at 0.2 M concentration promote the assembly on graphite, an ill-defined process in their absence. Also, after only three bilayers, the current densities are 7.3 (Cl^-) and 9.8 (Br^-) μA cm^{-2} in the absence of glucose and 233 (Cl^-) and 570 (Br^-) μA cm^{-2} in the presence of glucose. In the case of bromide, the catalytic current is comparable with those obtained with systems built using polyelectrolytes containing tethers binding redox centers to linear polymer backbones,[35,36] using less material and a redox polyelectrolyte obtained by a simpler synthesis. For example, Godman et al.,[35] with four bilayers of a ferrocene-modified linear PEI and GOx, obtained a maximum catalytic current of ca. 300 μA cm^{-2}, while Mao et al.[36] adding tethers binding redox centers to polyvinylpyridine through a laborious synthetic method obtained a catalytic current density of 1150 μA cm^{-2}. In this last case, the current density is calculated from an experiment where a microelectrode is used, and therefore, the mass transfer process is optimized.

The ratio between current densities in the presence and the absence of glucose can be used as an estimator of the rate constant for the electron transfer reaction between the mediator and the enzyme. The ratio between catalytic and noncatalytic currents obtained for bromide is close to the ratio observed for OsPAA containing gold nanoparticles and

https://doi.org/10.1021/acsapm.2c01300
ACS Appl. Polym. Mater. XXXX, XXX, XXX−XXX

dodecylsulfate, 59 (Br^-) versus 90 (dodecylsulfate), respectively; however, in that case, a thinner film was prepared, and therefore, a smaller catalytic current was observed (ca. 50 $\mu A\ cm^{-2}$).[32]

Using QCM-D and PM-IRRAS, it was possible to establish the amount of the polyelectrolyte and enzyme adsorbed in each layer and the effect of the presence of the salt in the construction process. Combining both techniques, it was possible to determine that GOx can be adsorbed from an aqueous solution at pH 7.0, while a consecutive exposition to the polyelectrolyte doped with the salt produces a rinsing effect, removing part of the enzyme and adsorbing a new OsPEI layer. This process can be understood considering the model proposed by Fu and Schlenoff,[5] in which the generation of polyelectrolyte complexes on multilayer systems is mainly driven by an entropic effect, where the GOx exposure to a doped polyelectrolyte layer produces an exchange, releasing the small anions and adsorbing GOx. In the following step, a more complex mechanism is involved, where a part of GOx loosely adsorbed is removed by the ionic strength of the polyelectrolyte solution, and the doped polyelectrolyte is adsorbed due to hydrophobic interaction with the enzyme and liberation of positive ions (Na^+).

The mass balances for the two systems (Table 1) show that a higher amount of the mass is adsorbed in the presence of bromide, indicating the relevance of the nature of the ion, while the mass ratio between GOx and OsPEI is practically the same (2.4) for both anions. This ratio is another piece of evidence supporting the idea that the presence of bromide generates a hydrogel with better interactions between the enzyme and mediator. This can be explained considering the structure of the film by analyzing the relative dissipation change ($-\Delta D/\Delta F$), where greater changes are observed for bromide, indicative of a more flexible film, which in turn improves the interaction between osmium centers and flavin adenine dinucleotide (FAD) cofactors buried in the enzyme. On the other hand, AFM data reveal the hydrophobic character of the bromide anion as it (1) enhances the interaction between the polymer and the hydrophobic HOPG surface and (2) causes bulky adsorption of the polymer over a gold surface, which is indicative of a strong polymer−polymer interaction.

The concentration of the anion has a similar effect to that observed in other works.[6,28,39,40] In the case of bromide, the amount of the adsorbed mass increases up to a certain concentration and then decays due to the screening effect of the same ions. The maximum is observed in the range of 0.2−0.5 M. Then, the electrochemical response decays abruptly at 0.8 M. On the other hand, the maximum current densities for chloride appear at a higher concentration (1 M). This can be ascribed to the fact that the doping of the polyelectrolyte takes place at a higher concentration than bromide, and therefore, the screening effect begins to prevail at higher concentrations. These results agree with those from the study by Yang et al.[6] reported for the PDADMAC/PSS polyelectrolyte complex (PEC) with several salts. They report that there is a maximum concentration where these ions act as counterions and the most hydrophobic ions reach this stage at lower values.

For OsPAA, a linear polyelectrolyte, the same trend is observed regarding the chemical nature of the ion. Adsorption of the redox polyelectrolyte is higher in this system, and the GOx/enzyme ratio is strikingly higher (with Br^-: 14 vs 2.4 for OsPEI), even though this is not reflected in a better catalytic current. The relative dissipation ($-\Delta D/\Delta F$) observed here is smaller and with the opposite sign compared to that of OsPEI, indicating a more rigid system, which can affect the electron transfer process between GOx and the osmium complex. Also, the greater amount of GOx present in the film can act as an insulator due to the formation of enzyme clusters. It is important to highlight that for both redox polyelectrolytes, the presence of bromide in the construction process yields systems with higher catalytic currents, leading to the conclusion that GOx adsorption is heavily dependent on the hydrophobic character of the precedent layer. Also, the OsPAA ion doping has a striking effect on graphite electrodes in the adsorption process and in the catalysis; the current observed here, 240 $\mu A\ cm^{-2}$, is 2.5 times higher than those observed with OsPAA in the presence of phosphate, gold nanoparticles, surfactants, and their combinations.[33,34,41]

Finally, the use of enzyme-redox hydrogel modified electrodes as bioanodes in enzymatic fuel cells has shown outstanding performance for this type of fuel cell, mainly devoted to self-powered implantable medical devices. In this type of cell, a size reduction is extremely important. In this work, by combining our assembly process (OsPEI@NaBr/GOx@H_2O) with a carbon cloth as an electrode, we obtain a higher power output compared to that of most enzymatic fuel cells recently presented in the literature (Table 2).

Table 2. Comparison of the Maximum Power Density Output (P_{max}) for Biofuel Cells

biofuel cell features	P_{max} ($mW\ cm^{-2}$)	references
mediator entrapped in polyelectrolyte	$8 \times 10-^5$	4
enzyme cascade based biofuel cell	0.04	45
self-assembled ferrocene−CNT−GOx	0.09	46
paper based biofuel cell	0.10	47
self-powered diaper sensor	0.12	48
self-assembled enzyme-redox polyelectrolyte	0.15	21
FAD-glucose dehydrogenase biofuel cell	0.27	49
increased real surface using graphene	0.38	50
N-doped CNTS@C_3N_4 network	0.57	51
stacked biofuel cell	0.58	52
gas-diffusion biocathode	0.66	53
gold nanoparticle-modified carbon nanotube	1.2	43
gold nanoparticles are LbL assembled with small organic linkers	3.7	44
biofuel cells with circular electrodes distribution	4.7	54
glucose oxidase is repeatedly assembled with hydrophobic metal nanoparticles	7.3	42
$(OsPEI@NaBr/GOx)_3$	2.46	this work
$(OsPAA@NaBr/GOx)_3$	0.80	this work

The results obtained by Kwon's group[42−44] correspond to biofuel cells where direct electron transfer is obtained by combining GOx with gold nanoparticles (AuNP), which requires a highly porous architecture for an efficient current output involving an amount of AuNP and enzyme that surpasses several times the amount of polyelectrolyte and enzyme used in this work. On the other hand, MET, a process in which electrons are shuttled between the enzyme and electrode by redox moieties, is able to build multilayers connecting more molecules of the enzyme, multiplying by several times the current obtained. The immobilization on the electrode surface and the interaction among the redox centers (redox shuttle and enzyme cofactor) is key to obtaining an

https://doi.org/10.1021/acsapm.2c01300
ACS Appl. Polym. Mater. XXXX, XXX, XXX−XXX

effective electron transport through the film and then transfer to the electrode. Previous studies by our group show that the introduction of surfactants enhances the hydrophobic characteristics of the redox polyelectrolyte, allowing better adsorption of the film on practically any surface, and improves the enzyme adsorption and the interaction between the enzyme and polyelectrolyte.[41] Recently, Yang et al.[6] studied the effect of the nature of the doping anions on the behavior of polyelectrolyte complexes. As the anion becomes more hydrophobic, its ability to ion pair with the positively charged polyelectrolyte increases and therefore its hydrophobic character. In this work, this phenomenon was exploited to improve the adsorption on different surfaces (graphite, gold, and carbon felt) and the interaction with GOx, as it can be observed by the obtained currents, the amount and ratio of the polyelectrolyte and enzyme adsorbed, and the AFM data, revealing the hydrophobic characteristics given by the bromide ion. Fine-tuning the anion and polyelectrolyte used should be considered. More hydrophobic anions, like perchlorate, transform the polyelectrolyte into an intractable material, while a more hydrophilic anion reduces the interaction between the polyelectrolyte and the enzyme due to an increase in free volume as it was proposed for polyelectrolyte complexes.[6] On the other hand, even though bromide-doped PAA has shown a higher adsorption of GOx, the result is an insulation effect with a lower catalytic current.

CONCLUSIONS

The presence of salts and their nature play an outstanding role in the assembly buildup. Branched PEI was demonstrated to be a more suitable polyelectrolyte for electrode modification since a higher power density output can be obtained with less material adsorbed onto the electrode, ascribable to its more flexible character and better interaction. With the use of a more hydrophobic anion such as the bromide ion, a greater amount of the redox polyelectrolyte and enzyme is adsorbed, and higher catalytic and non-catalytic current densities and more efficient electron transfer between redox centers in the hydrogel are obtained. Also, the combination of QCM-D, PM-IRRAS, and AFM allows understanding of the buildup mechanism of these films, shedding light on the effect of these doping anions on the characteristics of the film and its effect on the electron transfer process. This study not only introduces new evidence regarding the mechanism governing protein adsorption on polyelectrolytes but also offers a new strategy for the design of enzymatic-based bioanodes with an outstanding performance compared to similar enzymatic fuel cells.[35,46,55,56] We plan long-term performance studies and the replacement of osmium for a more economical and environmentally friendly source as future steps in this development.

ASSOCIATED CONTENT

Supporting Information

The Supporting Information is available free of charge at https://pubs.acs.org/doi/10.1021/acsapm.2c01300.

OsPEI/GOx assembly with other salts; peak current densities for cyclic voltammetry measurements carried out at 10 mV s^{-1} after deposition of each bilayer OsPEI/GOx in the absence and presence of glucose; PM-IRRA spectra of a gold surface modified with the assembly OsPEI/GOx using OsPEI solutions with 0.2 M NaBr and NaCl; AFM images of OsPEI/GOx films with NaCl and NaBr; peak current densities for cyclic voltammetry measurements carried out at 10 mV s^{-1} after deposition of each bilayer in the absence of glucose; maximum catalytic current densities in the presence of glucose; PM-IRRA spectra of the gold sample modified with the OsPAA/GOx assembly; variations in the intensity of the main signal in the PM-IRRA spectra as a function of layer increment; and mass adsorbed change, dissipation change, relative dissipation change, and thickness of each layer of the assembled OsPEI/GOx and OsPAA/GOx (PDF)

AUTHOR INFORMATION

Corresponding Author

Fernando Battaglini − *INQUIMAE (CONICET), Departamento de Química Inorgánica, Analítica y Química Física, Facultad de Ciencias Exactas y Naturales, Universidad de Buenos Aires, C1428EHA Buenos Aires, Argentina;* orcid.org/0000-0002-1113-1642; Phone: +541152858299; Email: battagli@qi.fcen.uba.ar; Fax: +541145763341

Authors

Lucy L. Coria-Oriundo − *INQUIMAE (CONICET), Departamento de Química Inorgánica, Analítica y Química Física, Facultad de Ciencias Exactas y Naturales, Universidad de Buenos Aires, C1428EHA Buenos Aires, Argentina;* orcid.org/0000-0003-3502-4726

Santiago E. Herrera − *INQUIMAE (CONICET), Departamento de Química Inorgánica, Analítica y Química Física, Facultad de Ciencias Exactas y Naturales, Universidad de Buenos Aires, C1428EHA Buenos Aires, Argentina;* orcid.org/0000-0002-8327-3914

Lucila P. Méndez De Leo − *INQUIMAE (CONICET), Departamento de Química Inorgánica, Analítica y Química Física, Facultad de Ciencias Exactas y Naturales, Universidad de Buenos Aires, C1428EHA Buenos Aires, Argentina;* orcid.org/0000-0003-4969-8078

Complete contact information is available at: https://pubs.acs.org/10.1021/acsapm.2c01300

Author Contributions

L.L.C.-O. conceptualized the project, performed investigations, developed the methodology, conducted formal analysis, and wrote the original draft. S.E.H. conceptualized the project, developed the methodology, and conducted formal analysis. L.P.M.d.L. conceptualized the project, developed the methodology, and conducted formal analysis. F.B. conceptualized the project, conducted formal analysis and supervision, and wrote and edited the manuscript.

Funding

F.B. received funding from ANPCYT, Argentina (PRESTAMO BID-PICT NRO 2018-02075), Universidad de Buenos Aires (UBACYT grant 0020170100341BA), and CONICET (grant KE5 11220200101473CO).

Notes

The authors declare no competing financial interest.

ACKNOWLEDGMENTS

L.L.C.O. acknowledges CONICET for financial support. S.E.H., L.M.D.L., and F.B. are research staff of CONICET.

REFERENCES

(1) Kucherenko, I. S.; Soldatkin, O. O.; Dzyadevych, S. V.; Soldatkin, A. P. Electrochemical biosensors based on multienzyme systems: main groups, advantages and limitations − A Review. *Anal. Chim. Acta* **2020**, *1111*, 114−131.

(2) Sharifi, M.; Pothu, R.; Boddula, R.; Bardajee, G. R. Trends of biofuel cells for smart biomedical devices. *Int. J. Hydrogen Energy* **2021**, *46*, 3220−3229.

(3) Heller, A.; Feldman, B. Electrochemistry in diabetes management. *Acc. Chem. Res.* **2010**, *43*, 963−973.

(4) Lim, K.; Lee, Y. S.; Simoska, O.; Dong, F.; Sima, M.; Stewart, R. J.; Minteer, S. D. Rapid entrapment of phenazine ethosulfate within a polyelectrolyte complex on electrodes for efficient NAD^+ regeneration in mediated NAD^+-dependent bioelectrocatalysis. *ACS Appl. Mater. Interfaces* **2021**, *13*, 10942−10951.

(5) Fu, J.; Schlenoff, J. B. Driving forces for oppositely charged polyion association in aqueous solutions: enthalpic, entropic, but not electrostatic. *J. Am. Chem. Soc.* **2016**, *138*, 980−990.

(6) Yang, M.; Digby, Z. A.; Schlenoff, J. B. Precision doping of polyelectrolyte complexes: insight on the role of ions. *Macromolecules* **2020**, *53*, 5465−5474.

(7) Omidvar, M.; Zdarta, J.; Sigurdardóttir, S. B.; Pinelo, M. Mimicking natural strategies to create multi-environment enzymatic reactors: from natural cell compartments to artificial polyelectrolyte reactors. *Biotechnol. Adv.* **2022**, *54*, 107798.

(8) Rončević, I. Š.; Krivić, D.; Buljac, M.; Vladislavić, N.; Buzuk, M. Polyelectrolytes assembly: A powerful tool for electrochemical sensing application. *Sensors* **2020**, *20*, 3211.

(9) vander Straeten, A.; Lefèvre, D.; Demoustier-Champagne, S.; Dupont-Gillain, C. Protein-based polyelectrolyte multilayers. *Adv. Colloid Interface Sci.* **2020**, *280*, 102161.

(10) He, P.; Hu, N. Interactions between heme proteins and dextran sulfate in layer-by-layer assembly films. *J. Phys. Chem. B* **2004**, *108*, 13144−13152.

(11) Yang, X.; Zhang, H.; Yuan, X.; Cui, S. Wool keratin: A novel building block for layer-by-layer self-assembly. *J. Colloid Interface Sci.* **2009**, *336*, 756−760.

(12) Art, J. F.; vander Straeten, A.; Dupont-Gillain, C. C. Immobilization of aluminum hydroxide particles on quartz crystal microbalance sensors to elucidate antigen−adjuvant interaction mechanisms in vaccines. *Anal. Chem.* **2018**, *90*, 1168−1176.

(13) Müller, M.; Rieser, T.; Dubin, P. L.; Lunkwitz, K. Selective interaction between proteins and the outermost surface of polyelectrolyte multilayers: influence of the polyanion type, pH and salt. *Macromol. Rapid Commun.* **2001**, *22*, 390−395.

(14) Baldwin, R. L. How Hofmeister ion interactions affect protein stability. *Biophys. J.* **1996**, *71*, 2056−2063.

(15) Schaaf, P.; Schlenoff, J. B. Saloplastics: Processing compact polyelectrolyte complexes. *Adv. Mater.* **2015**, *27*, 2420−2432.

(16) Zhang, Y.; Cremer, P. S. Interactions between macromolecules and ions: The Hofmeister series. *Current Opinion in Chemical Biology*; Elsevier Current Trends, 2006; Vol. *10*, pp 658−663.

(17) He, Q.; Huang, Y.; Wang, S. Hofmeister effect-assisted one step fabrication of ductile and strong gelatin hydrogels. *Adv. Funct. Mater.* **2018**, *28*, 1705069.

(18) Rogers, B. A.; Okur, H. I.; Yan, C.; Yang, T.; Heyda, J.; Cremer, P. S. Weakly hydrated anions bind to polymers but not monomers in aqueous solutions. *Nat. Chem.* **2022**, *14*, 40−45.

(19) Hua, M.; Wu, S.; Ma, Y.; Zhao, Y.; Chen, Z.; Frenkel, I.; Strzalka, J.; Zhou, H.; Zhu, X.; He, X. Strong tough hydrogels via the synergy of freeze-casting and salting out. *Nature* **2021**, *590*, 594−599.

(20) Kober, E. M.; Caspar, J. V.; Sullivan, B. P.; Meyer, T. J. Synthetic routes to new polypyridyl complex of Osmium(II). *Inorg. Chem.* **1988**, *27*, 4587−4598.

(21) Coria-Oriundo, L. L.; Cortez, M. L.; Azzaroni, O.; Battaglini, F. Enzymes hosted in redox-active ionically cross-linked polyelectrolyte networks enable more efficient biofuel cells. *Soft Matter* **2021**, *17*, 5240−5247.

(22) Hermanson, G. T. Part III: Bioconjugate Applications. *Bioconjugate Techniques*; Academic Press, 1996; pp 419−455.

(23) Priano, G.; González, G.; Günther, M.; Battaglini, F. Disposable gold electrode array for simultaneous electrochemical studies. *Electroanalysis* **2008**, *20*, 91−97.

(24) Rivas, M. V.; De Leo, L. P.; Hamer, M.; Carballo, R.; Williams, F. J. Self-assembled monolayers of disulfide cu porphyrins on au surfaces: adsorption induced reduction and demetalation. *Langmuir* **2011**, *27*, 10714−10721.

(25) Kou, R.; Zhang, J.; Chen, Z.; Liu, G. Counterion specificity of polyelectrolyte brushes: role of specific ion-pairing interactions. *ChemPhysChem* **2018**, *19*, 1404−1413.

(26) Barth, A. Infrared spectroscopy of proteins. *Biochim. Biophys. Acta, Bioenerg.* **2007**, *1767*, 1073−1101.

(27) Lojou, E.; Bianco, P. Key Role of the anchoring PEI layer on the electrochemistry of redox proteins at carbon electrodes. consequences on assemblies involving proteins and clay. *Electrochim. Acta* **2007**, *52*, 7307−7314.

(28) Dressick, W. J.; Wahl, K. J.; Bassim, N. D.; Stroud, R. M.; Petrovykh, D. Y. Divalent-anion salt effects in polyelectrolyte multilayer depositions. *Langmuir* **2012**, *28*, 15831−15843.

(29) El Haitami, A. E.; Martel, D.; Ball, V.; Nguyen, H. C.; Gonthier, E.; Labbé, P.; Voegel, J.-C.; Schaaf, P.; Senger, B.; Boulmedais, F. Effect of the supporting electrolyte anion on the thickness of PSS/PAH multilayer films and on their permeability to an electroactive probe. *Langmuir* **2009**, *25*, 2282−2289.

(30) Tagliazucchi, M.; Grumelli, D.; Calvo, E. J. Nanostructured modified electrodes: Role of ions and solvent flux in redox active polyelectrolyte multilayer films. *Phys. Chem. Chem. Phys.* **2006**, *8*, 5086−5095.

(31) Yokota, S.; Ueno, T.; Kitaoka, T.; Tatsumi, D.; Wariishi, H. Morphological imaging of single methylcellulose chains and their thermoresponsive assembly on a highly oriented pyrolytic graphite surface. *Biomacromolecules* **2007**, *8*, 3848−3852.

(32) Cortez, M. L.; Marmisollé, W.; Pallarola, D.; Pietrasanta, L. I.; Murgida, D. H.; Ceolín, M.; Azzaroni, O.; Battaglini, F. Effect of gold nanoparticles on the structure and electron-transfer characteristics of glucose oxidase redox polyelectrolyte-surfactant complexes. *Chem. - Eur. J.* **2014**, *20*, 13366−13374.

(33) Cortez, M. L. M. L.; Cukierman, A. L. A. L.; Battaglini, F. Surfactant presence in a multilayer polyelectrolyte-enzyme system improves its catalytic response. *Electrochem. Commun.* **2009**, *11*, 990−993.

(34) Zappi, D.; Coria-Oriundo, L. L.; Piccinini, E.; Gramajo, M.; von Bilderling, C.; Pietrasanta, L. I.; Azzaroni, O.; Battaglini, F. The effect of ionic strength and phosphate ions on the construction of redox polyelectrolyte−enzyme self-assemblies. *Phys. Chem. Chem. Phys.* **2019**, *21*, 22947−22954.

(35) Godman, N. P.; DeLuca, J. L.; McCollum, S. R.; Schmidtke, D. W.; Glatzhofer, D. T. Electrochemical characterization of layer-by-layer assembled ferrocene-modified linear poly(ethylenimine)/enzyme bioanodes for glucose sensor and biofuel cell applications. *Langmuir* **2016**, *32*, 3541−3551.

(36) Mao, F.; Mano, N.; Heller, A. Long tethers binding redox centers to polymer backbones enhance electron transport in enzyme "wiring" hydrogels. *J. Am. Chem. Soc.* **2003**, *125*, 4951−4957.

(37) Salomäki, M.; Tervasmäki, P.; Areva, S.; Kankare, J. The Hofmeister anion effect and the growth of polyelectrolyte multilayers. *Langmuir* **2004**, *20*, 3679−3683.

(38) Salomäki, M.; Laiho, T.; Kankare, J. Counteranion-controlled properties of polyelectrolyte multilayers. *Macromolecules* **2004**, *37*, 9585−9590.

(39) Decher, G.; Schlenoff, J. B. *Multilayer Thin Films: Sequential Assembly of Nanocomposite Materials*; Decher, G., Schlenoff, J. B., Eds.; Wiley, 2012; Vol. *1*−*2*.

(40) Digby, Z. A.; Yang, M.; Lteif, S.; Schlenoff, J. B. Salt resistance as a measure of the strength of polyelectrolyte complexation. *Macromolecules* **2022**, *55*, 978.

https://doi.org/10.1021/acsapm.2c01300
ACS Appl. Polym. Mater. XXXX, XXX, XXX−XXX

(41) Cortez, M. L.; Ceolín, M.; Cuellar Camacho, L.; Donath, E.; Moya, S. E.; Battaglini, F.; Azzaroni, O. Solvent effects on the structure−property relationship of redox-active self-assembled nanoparticle−polyelectrolyte−surfactant composite thin films: implications for the generation of bioelectrocatalytic signals in enzyme-containing assemblies. *ACS Appl. Mater. Interfaces* **2017**, *9*, 1119−1128.
(42) Kwon, C. H.; Kang, M.; Kwon, M.; Nam, D.; Song, Y.; Yong, E.; Oh, M.-K.; Kim, Y.; Yeom, B.; Moon, J. H.; Lee, S. W.; Cho, J. High-performance hybrid biofuel cells using amphiphilic assembly based enzyme electrodes. *Appl. Phys. Rev.* **2022**, *9*, 021413.
(43) Kwon, C. H.; Ko, Y.; Shin, D.; Lee, S. W.; Cho, J. Highly conductive electrocatalytic gold nanoparticle-assembled carbon fiber electrode for high-performance glucose-based biofuel cells. *J. Mater. Chem. A* **2019**, *7*, 13495−13505.
(44) Kwon, C. H.; Ko, Y.; Shin, D.; Kwon, M.; Park, J.; Bae, W. K.; Lee, S. W.; Cho, J. High-power hybrid biofuel cells using layer-by-layer assembled glucose oxidase-coated metallic cotton fibers. *Nat. Commun.* **2018**, *9*, 4479.
(45) Fan, S.; Liang, B.; Xiao, X.; Bai, L.; Tang, X.; Lojou, E.; Cosnier, S.; Liu, A. Controllable display of sequential enzymes on yeast surface with enhanced biocatalytic activity toward efficient enzymatic biofuel cells. *J. Am. Chem. Soc.* **2020**, *142*, 3222−3230.
(46) Bahar, T.; Yazici, M. S. Immobilized glucose oxidase biofuel cell anode by MWCNTs, ferrocene, and polyethylenimine: Electrochemical performance. *Asia-Pac. J. Chem. Eng.* **2018**, *13*, No. e2149.
(47) Kim, M.; Kwon, Y.; Ahn, Y. Paper-based mediatorless enzymatic microfluidic biofuel cells. *Biosens. Bioelectron.* **2021**, *190*, 113391.
(48) Shitanda, I.; Fujimura, Y.; Takarada, T.; Suzuki, R.; Aikawa, T.; Itagaki, M.; Tsujimura, S. Self-powered diaper sensor with wireless transmitter powered by paper-based biofuel cell with urine glucose as fuel. *ACS Sens.* **2021**, *6*, 3409−3415.
(49) Cohen, R.; Bitton, R. E.; Herzallh, N. S.; Cohen, Y.; Yehezkeli, O. Utilization of FAD-glucose dehydrogenase from *t. emersonii* for amperometric biosensing and biofuel cell devices. *Anal. Chem.* **2021**, *93*, 11585−11591.
(50) Lee, J.; Hyun, K.; Park, J. M.; Park, H. S.; Kwon, Y. Maximizing the enzyme immobilization of enzymatic glucose biofuel cells through hierarchically structured reduced graphene oxide. *Int. J. Energy Res.* **2021**, *45*, 20959−20969.
(51) Li, G.; Ren, G.; Wang, W.; Hu, Z.; Hu, Z. Rational design of N-doped CNTs@C_3N_4 network for dual-capture of biocatalysts in enzymatic glucose/O_2 biofuel cells. *Nanoscale* **2021**, *13*, 7774−7782.
(52) Escalona-Villalpando, R. A.; Hasan, K.; Milton, R. D.; Moreno-Zuria, A.; Arriaga, L. G.; Minteer, S. D.; Ledesma-García, J. Performance comparison of different configurations of glucose/O_2 microfluidic biofuel cell stack. *J. Power Sources* **2019**, *414*, 150−157.
(53) Tatara, R.; Sakai, S.; Horiba, T.; Komaba, S. Impact of surface hydrophilicity of gas-diffusion-type biocathodes on their oxygen reduction ability for biofuel cells. *J. Electrochem. Soc.* **2021**, *168*, 074506.
(54) Huang, X.; Zhang, J.; Su, H.; Sun, F.; Lu, Z.; Su, A.; Liu, J. Exploring the shape and distribution of electrodes in membraneless enzymatic biofuel cells for high power output. *Int. J. Hydrogen Energy* **2021**, *46*, 17414−17420.
(55) Liu, J.; Zhang, X.; Pang, H.; Liu, B.; Zou, Q.; Chen, J. High-performance bioanode based on the composite of CNTs-immobilized mediator and silk film-immobilized glucose oxidase for glucose/O_2 biofuel cells. *Biosens. Bioelectron.* **2012**, *31*, 170−175.
(56) Hickey, D. P.; Giroud, F.; Schmidtke, D. W.; Glatzhofer, D. T.; Minteer, S. D. Enzyme cascade for catalyzing sucrose oxidation in a biofuel cell. *ACS Catal.* **2013**, *3*, 2729−2737.

https://doi.org/10.1021/acsapm.2c01300
ACS Appl. Polym. Mater. XXXX, XXX, XXX−XXX